Journal of Clinical and Translational Hepatology **2022**
DOI: 10.14218/JCTH.2022.00276

Original Article

STX5 Inhibits Hepatocellular Carcinoma Adhesion and Promotes Metastasis by Regulating the PI3K/mTOR Pathway

Bin Zhang[1,2], Ziyin Zhao[2], Youpeng Wang[3], Tingting Guo[3], Mingyang He[2], Ge Guan[2], Pai Peng[2], Jinzhen Cai[2], Bingyuan Zhang[3], Xutao Liu[4] and Qiaoling Song[1*]

[1]Key Laboratory of Marine Drugs, Ministry of Education School of Medicine & Pharmacy, Ocean University of China, Qingdao, Shandong, China; [2]Organ Transplantation Center, The Affiliated Hospital of Qingdao University, Qingdao, Shandong, China; [3]Department of Hepatobiliary and Pancreatic Surgery, The Affiliated Hospital of Qingdao University, Qingdao, Shandong, China; [4]Samueli School of Engineering, University of California Los Angeles, Los Angeles, CA, USA

Received: 5 June 2022 | **Revised:** 21 July 2022 | **Accepted:** 15 August 2022 | **Published:** 9 January 2023

Abstract

Background and Aims: Syntaxin 5 (STX5) is a member of the syntaxin or target-soluble SNAP receptor (t-SNARE) family and plays a critical role in autophagy. However, its function and molecular mechanism in tumor cell migration are still unknown. The role of STX5 in influencing hepatocellular carcinoma (HCC) is an important topic in our research. ***Methods:*** By using quantitative reverse transcription polymerase chain reaction (qPCR), western blotting, and immunohistochemical analysis of RNA and protein in tissues, we comprehensively evaluated data sets from public databases and clinical patient cohorts for STX5. The correlation of STX5 expression with the clinicopathological characteristics of HCC patients were assessed. In addition, we predicted signal pathways from differentially expressed genes (DEGs) and the Cancer Genome Atlas (TCGA) databases, and confirmed the prediction using integrated transcriptome and RNA-seq. We further investigated the underlying mechanisms of STX5 in the migration and adhesion of HCC cells both *in vitro* and *in vivo*. ***Results:*** In the TCGA dataset and our patient cohort, STX5 levels were significantly higher in HCC tissues than in adjacent normal liver tissues. At the same time, high expression of STX5 predicted worse prognosis in patients with liver cancer. High expression of STX5 indicates the decrease of adhesion and the increase of migration of HCC cells, and the conversion of epithelial-mesenchymal transition (EMT) *in vitro* via PI3K/mTOR pathway activation. Conversely, when Sirolimus, a phosphoinositide 3-kinase (PI3K)/AKT/mechanistic target of rapamycin (mTOR) inhibitor acts on cells simultaneously, STX5 overexpression-mediated enhancement of HCC metastasis is reversed. Double-negative regulation of STX5 and mTOR further enhanced the inhibitory effect of STX5 on HCC metastasis. *In vivo*, STX5 knockdown inhibited the metastasis of HCC cells. ***Conclusions:*** Our study demonstrates a novel research result that STX5 promotes HCC metastasis through PI3K/mTOR pathway. We believe that combined inhibition of STX5 and mTOR is a potential treatment for effectively prolonging patient survival and inhibiting HCC metastasis.

Citation of this article: Zhang B, Zhao Z, Wang Y, Guo T, He M, Guan G, *et al*. STX5 Inhibits Hepatocellular Carcinoma Adhesion and Promotes Metastasis by Regulating the PI3K/mTOR Pathway. J Clin Transl Hepatol 2022. doi: 10.14218/JCTH.2022.00276.

Introduction

The incidence and mortality of liver cancer have remained high in recent years. The age-standardized incidence rate is 17.64/100,000 among Chinese and 17.35/100,000 worldwide.[1,2] Liver cancer has the fourth highest mortality rate among cancers (8.3%).[3] Hepatocellular carcinoma (HCC) is the main pathological type of primary HCC, accounting for more than 75%. Several treatment modalities, including surgical resection, liver transplantation, ablation therapy, and treatment with targeted drugs such as sorafenib and lenvatinib, have somewhat improved the prognosis of HCC patients.[4] Although significant progress has recently been made in the long-term process of resisting HCC, it is characterized by high recurrence and metastasis rates of malignant tumors, which makes the long-term survival rate of patients a concern.[5] Consequently, effectively improving the prognosis of HCC continues to be a complex problem. Thus, identifying effective targets and developing new therapeutic strategies to prolong the survival of HCC patients are highly important.

A member of the syntaxin family, syntaxin 5 (STX 5) is the target of vesicle-soluble snap receptors (v-SNAREs) and allows specific synaptic vesicles to contact each other and fuse.[6,7] STX5 is a widely expressed one-way type IV membrane protein belonging to the syntaxin family. It is considered to act mainly in the intracellular transport of vesicles

Keywords: Syntaxin 5; Hepatocellular carcinoma; PI3K/mTOR; Epithelial-mesenchymal transition.

Abbreviations: AFP, alpha-fetoprotein; BCA, bicinchoninic acid; DCA, Decision curve analysis; DEGs, differentially expressed genes; DFS, disease-free survival; DMEM, Dulbecco's modified Eagle's medium; EMT, epithelial-mesenchymal transition; GSEA, Gene Set Enrichment Analysis; HBV, hepatitis B virus; HCC, hepatocellular carcinoma; IHC, Immunohistochemical; KEGG, Kyoto Encyclopedia of Genes and Genomes; OS, overall survival; PBS, phosphate buffered saline; PVDF, polyvinylidene difluoride; qPCR, quantitative polymerase chain reaction; STX5, Syntaxin 5; TCGA, the Cancer Genome Atlas.

***Correspondence to:** Qiaoling Song, Key Laboratory of Marine Drugs, Ministry of Education School of Medicine & Pharmacy, Ocean University of China, Qingdao, Shandong 266071, China. ORCID: https://orcid.org/0000-0003-1389-9433. Tel: +86-532-86906810, Fax: +86-532-66782151, E-mail: sql_simm@163.com

as a soluble N-ethylmaleimide-sensitive factor attachment receptor (SNARE) protein.[8] STX5 is localized mainly in the endoplasmic reticulum, the cis-Golgi cisterna in the early secretory pathway, and the endoplasmic reticulum–Golgi intermediate compartment,[9] and it plays an important role in regulating transport from endoplasmic reticulum to Golgi apparatus.[10,11] The function of STX5 is critical for the formation of endoplasmic reticulum-derived transport vesicles and their transport to the Golgi apparatus, as well as for intracellular vesicle tubule fusion and the formation of cis-Golgi pools.[12] STX5 thus participates in intracellular vesicle transport.[13] Moreover, it is necessary for maintaining the structure of the Golgi apparatus.[14] In summary, STX5 encodes proteins that regulate transport from the endoplasmic reticulum to the Golgi apparatus, has key roles in autophagy, and is essential to many biological processes.

To date, no studies have reported the direct link between STX5 and tumors. However, the biological process in which it participates cannot be ignored in the development of tumors. It has been reported that STX5 has a considerable influence on autophagy.[15,16] In the process of HCC proliferation and metastasis, alpha-fetoprotein (AFP) regulates the expansion and migration of HCC cells, most likely mediated by phosphatidylinositol-3 kinase (PI3K)/mammalian target of rapamycin (mTOR).[17] The autophagy of HCC cells and the PI3K/mTOR pathway play an important role in HCC escape. However, little is known about whether STX5 is related to these pathways and whether it can affect migration, adhesion, epithelial-mesenchymal transition (EMT), and other behaviors in HCC cells.

In this study, the expression level of STX5 in HCC patients was determined. The clinicopathological characteristics of STX5, including patient survival, were carefully documented. STX5 and HCC cell migration, adhesion, and EMT transformation were experimentally verified in HCC cell lines and animal models. The results demonstrated the function of STX5 in PI3K/mTOR pathway-mediated HCC cell adhesion, migration, and EMT, which in turn affected metastatic HCC cells *in vitro* and *in vivo*.

Methods

Patients and specimens

Eight fresh HCC specimens and samples of normal tissues adjacent to surgically resected tissues were obtained at the Affiliated Hospital of Qingdao University between May and September 2021 and were used for protein extraction. Some of the specimens were stored at −80°C after surgical removal and those that remained were fixed in 10% formalin and embedded in paraffin. All samples were evaluated and histologically diagnosed.

Immunohistochemical (IHC) analysis

IHC staining was done on 116 paraffin-embedded HCC tissues collected at the Affiliated Hospital of Qingdao University between January 2015 and December 2016 to determine the level of STX5 protein expression. On the basis of the brightness of staining (0=negative, 1=weak, 2=medium, or 3=strong) and the percentage of strongly stained cells within the observed field (0=0%, 1=1–25%, 2=26–50%, and 3≥51%), scoring of IHC staining were multiplied by brightness and percentage scores. A final score of <4 was defined as low expression and a score of 4–9 was defined as high expression. Chi-square tests were used to determine the correlations between STX5 expression levels and the clinicopathological characteristics of HCC patients.

Cell culture

HL-7702 normal human liver cells and four HCC cell lines (Huh7, PLC/PRF/5, MHCC97H, and Hep3B) were bought from the Chinese Academy of Sciences (Shanghai, China). Cells were grown at 37°C in a 5% CO_2 atmosphere and cultured in Dulbecco's modified Eagle's medium (DMEM) with 10% fetal bovine serum (FBS) and 1% penicillin/streptomycin.

Transfection

An STX5 short hairpin (sh)RNA interference lentiviral vector was constructed and synthesized for stable transfection. An STX5 overexpression (OE-STX5) plasmid and empty (negative control) vector were also constructed. The lentiviral vectors were transduced into Huh7 and PLC/PRF/5 cells, and the expression plasmids were transfected into MHCC97H cells. HEK293T cells were used to conduct preliminary transfection experiments in 96-well plates to determine the appropriate multiplicity of infection value. The HCC cell lines were the used for formal transfection.

RNA extraction and quantitative real-time polymerase chain reaction (qPCR)

Whole-cell RNA was isolated using RNA-easy isolation reagent (Vazyme, Nanjing, China). PrimeScript RT Kits (TaKaRa, Otsu, Japan) were used to reverse-transcribe the extracted RNA into cDNA. TB Green Premix Ex Taq II, primers and cDNA were successively added according to the calculated results. qPCR was performed in an FTC-3000p real-time PCR system (Funglyn Biotech, Shanghai, China).

Western blot assay

Proteins were extracted from cells or tissues and resolved using RIPA lysis buffer. The protein concentration was measured with a bicinchoninic acid (BCA) assay kit and an enzyme-labeling instrument. Following 10 m incubation at 95°C, the protein lysates (20 μg) were separated using sodium lauryl sulfate-polyacrylamide gel electrophoresis and transferred to polyvinylidene difluoride (PVDF) membranes. After blocking with 5% defatted milk, the membranes were incubated with a specific primary antibody at 4°C for approximately 12 h. The membranes were then incubated with the secondary antibody at room temperature for around 1.5 h. An enhanced chemiluminescence system was used to read the protein bands. The primary antibodies were anti-p-PI3K, PI3K, mTOR, E-cadherin, N-cadherin, Vimentin, Snail, and GAPDH (Cell Signaling Technology, Danvers, MA, USA), and anti-STX5 (Abcam, Cambridge, UK).

Colony formation assay

Following treatment, cells were plated at 1,000 cells per well in six-well plates. Two weeks later, the cells were washed with phosphate buffered saline (PBS), fixed with 4% paraformaldehyde, stained with crystal violet solution for 30 m and washed again with PBS. The number of colonies in each sample was counted for statistical analysis.

Migration assay

To conduct the migration assay, Transwell chambers with 8 μm-pore membranes (Corning, NY, USA) were used. After transfection, a total of 5×10^4 cells were suspended in serum-free medium in the upper compartment and DMEM containing 30% FBS was placed in the lower compartment. The cells were incubated at 37°C for 24 h, fixed with 4% paraformaldehyde for 30 m, stained with 0.5% hexamethyl pararosaniline chloride for 20 m at room temperature, washed

with PBS to remove excess crystal violet, and counted by light microscopy (Nikon, Tokyo, Japan) in five fields.

Wound healing assay

In order to assess cell migration ability, wound healing assays were performed. Briefly, cells were plated in 6-well plates and cultured to more than 90% confluence. Then, a 200 μL pipette tip was used to scratch the surface. These cells were cultured in DMEM containing 2% FBS. Photographs of the wound area were taken with a light microscope (Nikon). The preparations were photographed at 0 and 48 h after wounding.

Cell adhesion assay

A 40 μg/mL collagen type I solution in PBS was prepared from calf skin and stored at 4°C. A 0.1% bovine albumin (BSA) solution was prepared in DMEM. The wells of 96-well plates were coated with collagen type I from calf skin (30 μL/well) at 4°C for 12 h. The solution was removed and the cells were deprived of serum for 8 h before the adhesion assay. The cells were cultured in DMEM after washing three times with serum-free DMEM and then collected in a solution of 10 mM EDTA in DMEM. Following a second wash with DMEM to remove the EDTA, the cells were resuspended in DMEM supplemented with 0.1% BSA at a density of 2×10^5 cells/mL. A 100 μL volume of the cell suspension was added to each well containing collagen type I. A 20 m incubation period at 37°C was used to allow the cells to adhere to the surface. Then, 100 μL of DMEM was added to each well to wash away any nonadherent cells. The adherent cells were washed four times, DMEM supplemented with 10% FBS was added, and the cells were incubated at 37°C for 4 h for recovery. CCK-8 reagent (10 μL) was then added to each well for about 2 h at 30°C. A 0.5% crystal violet solution was added for 20 m at room temperature and the absorbance was then measured at 490 nm with a spectrophotometer. Photography and counting of the stained cells were performed by light microscopy.

RNA sequencing (RNA-seq)

Huh7 cells were transfected with OE-STX5 and negative control plasmids for transcriptome sequencing, and functional enrichment analysis of the vector and OE-STX5 groups was performed. Each group of 1×10^7 cells were lysed with 1.5 mL of TRIzol reagent, repeatedly stirred with a syringe to make the solution clear and not viscous, and transported at −80°C. Libraries were constructed with NEBNext Ultra RNA Library Prep Kits (Illumina, San Diego, CA, USA). A Qubit 2.0 fluorometer, an Agilent 2100 Bioanalyzer, and qPCR were used for the quantification of effective concentrations in the library. After the library test qualification, computer sequencing was carried out.

In vivo experiments

In vivo experiments were conducted in accordance with the principles approved by the Animal Experiment Ethics Committee of Qingdao University. Male BALB/c nude mice of 4–6 weeks of age were purchased from the Charles River animal experiment center (Beijing, China). The mice were injected with 2×10^6 Huh7 LV-shNC cells or 2×10^6 Huh7 LV-shSTX5 cells suspended in 200 μL of PBS via the tail vein. The mice were housed in cages under standard conditions and were sacrificed 6 weeks after injection. The lungs were excised and embedded in paraffin for hematoxylin-eosin or IHC staining.

Bioinformatics analysis

We obtained gene expression data from The Cancer Genome Atlas (TCGA) database and analyzed the relationships between STX5 expression and HCC prognosis and clinical staging (https://portal.gdc.cancer.gov/projects/TCGA-LIHC). In addition, we analyzed the data using Gene Set Enrichment Analysis (GSEA). In order to provide a mensurable method for predicting the survival rate of HCC patients, we constructed a nomogram relying on STX5 and clinical parameters. Based on the transcriptome sequencing results, DisGeNET analysis and Kyoto Encyclopedia of Genes and Genomes (KEGG) enrichment analysis were used to analyze and forecast the function of STX5. The 335 HCC patients in the TCGA database with a follow-up of more than 0.1 year were divided into high STX5 expression (n=168) and low STX5 expression (n=167) groups.

Statistical analysis

We used SPSS version 23 (IBM Corp., Armonk, NY, USA) to perform the statistical analysis. P-values <0.05 indicated statistical significance. Kaplan-Meier survival analysis was conducted in combination with follow-up time and survival status.

Results

Compared with non-tumor liver tissues, STX5 protein was significantly overexpressed in HCC tissues

In the TCGA database, STX5 mRNA expression was significantly overexpressed in HCC tissues compared with non-tumor liver tissues (Fig. 1A). We confirmed this observation in matched frozen HCC and contiguous non-tumor liver tissues and observed prominent overexpression of STX5 in most HCC tissues (Fig. 1B). A total of 116 samples were assayed by IHC. The positive rate of liver cancer tissue was 81.8% (95/116) and that of paracancer tissue was 17.2% (20/116), which difference was statistically significant (Fig. 1D). 116 HCC patients were divided into low (n=55) and high(n=61) STX5 expression groups by immunohistochemical scores. There were significant differences in AFP level, hepatitis B virus (HBV) infection, and tumor number between the two groups (Table 1) (p<0.05).

High STX5 expression predicts a poor prognosis in HCC

Using datasets published in the TCGA database, we found that the median overall survival (OS) was significantly lower in HCC patients with high STX5 mRNA expression than in patients with low STX5 mRNA expression (Fig. 1C). Using the IHC scores of 116 patients, we found that compared with patients with low STX5 expression group, those with high STX5 expression had shorter OS and disease-free survival (DFS; Fig. 1E, F).

In HCC patients in TCGA, clinical grade was correlated with the STX5 expression level (Fig. 1G). Univariate and multivariate Cox regression analyses of the STX5 expression level, clinical grade, and clinical indicators in HCC patients in the TCGA database, further demonstrated that high STX5 expression was an independent risk factor for a poor prognosis in HCC (Fig. 1H). In addition, five independent prognostic factors were used to construct a nomogram for predicting 1-, 3-, and 5-year OS (Fig. 1I). Calibration plots were generated to compare the predicted and actual OS rates at the 1-, 3-, and 5-year follow-up (Fig. 1J).

Effects of STX5 expression on HCC cell adhesion, migration, and EMT

Further studies were performed to determine whether STX5 affected HCC cell adhesion, migration, and EMT in two HCC cell lines expressing high levels of STX5, Huh7 and PLC/PRF/5 (Fig. 2A, B). The cells were transduced with lentivi-

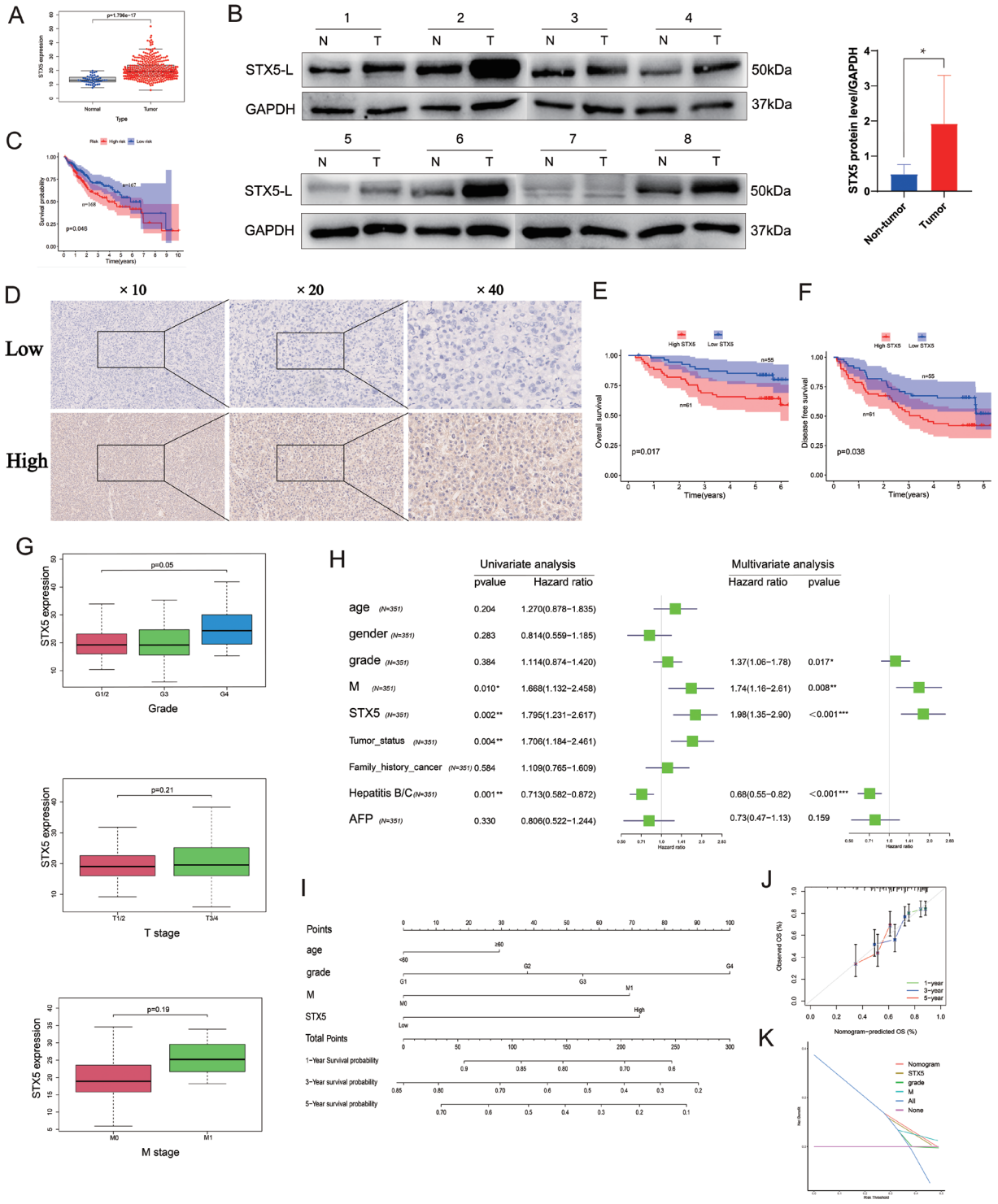

Fig. 1. Poor prognosis is linked to STX5 high expression in HCC. (A) Differences in STX5 mRNA expression between HCC tissues and tumor-adjacent tissues in patients with HCC in the TCGA database. Blue represents tumor-adjacent tissues, and red represents HCC tissue. (B) Western blot analysis compared STX5 protein expression in HCC and nontumor liver tissues with GAPDH expression levels as a normalization. (C) Correlation between STX5 mRNA expression and OS in HCC patients in the TCGA database. (D) Immunohistochemical analysis of STX5 protein expression in human HCC tissue. (E, F) STX5 protein expression in 116 patients with HCC was correlated with the OS and disease-free survival rates. (G) Correlation analysis of the STX5 expression level and clinical grade of HCC in patients in the TCGA database. (H) Univariate and multivariate Cox regression analyses of STX5 expression, clinical grade, and clinical indicators in HCC patients in the TCGA database. (I) Nomogram constructed based on five independent prognostic factors to predict 1-, 3-, and 5-year OS. (J) Calibration plots were generated to compare the predicted and actual OS probabilities at the 1-, 3-, and 5-year follow-up. (K) Decision curve analysis showed better clinical utility of the nomogram compared with other models of 3-year OS. STX5, Syntaxin 5; HCC, hepatocellular carcinoma; TCGA, the Cancer Genome Atlas; OS, overall survival; DCA, Decision curve analysis.

Table 1. Relevance analysis between STX5 expression and clinicopathological features in 116 patients with HCC

Variable	Number	STX5, n		χ^2	*P*-value
		Low	High		
Sex				0.043	0.836
Male	102	48	54		
Female	14	7	7		
Age (years)				0.005	0.946
<60	65	31	34		
≥60	51	24	27		
BMI				3.306	0.069
<24	53	30	23		
≥24	63	25	38		
Tumor size (cm)				0.143	0.706
<5	76	37	39		
≥5	40	18	22		
Liver cirrhosis				0.561	0.454
No	28	15	13		
Yes	88	40	48		
Microvascular invasion				0.639	0.424
No	78	39	39		
Yes	38	16	22		
Portal vein invasion				1.264	0.261
No	112	52	60		
Yes	4	3	1		
HBV				5.505	0.019
No	21	15	6		
Yes	95	41	54		
AFP level (ng/L)				4.041	0.044
<400	92	48	44		
≥400	24	7	17		
ALT level (U/L)				0.002	0.965
<60	93	44	49		
≥60	23	11	12		
AST (U/L)				1.483	0.223
<40	94	42	52		
≥40	22	13	9		
Tumor number				4.056	0.044
Single	97	50	47		
Multiple	19	5	14		
Alcohol abuse				3.274	0.070
No	76	40	36		
Yes	40	14	26		

Statistical assay of the association between STX5 expression and clinicopathological features of surgical HCC specimens is shown. *P*-values were calculated using χ^2 tests. Differences in AFP level, hepatitis B virus (HBV) infection, and tumor number were significant ($p<0.05$).

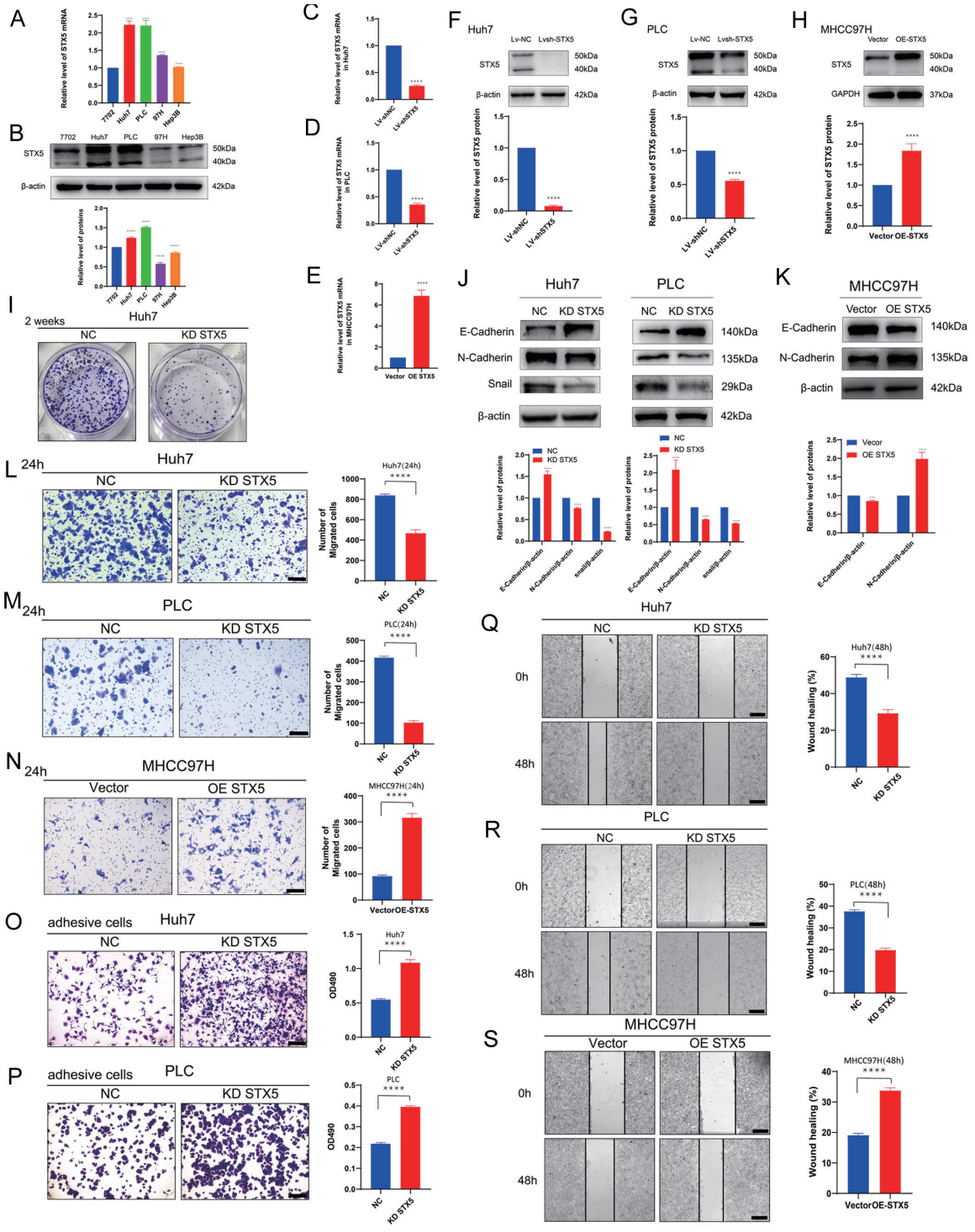

Fig. 2. Effects of STX5 expression level on HCC cell migration, adhesion, and EMT. (A) qPCR of basal STX5 mRNA expression in five cell lines. (B) Western blot analysis of basal STX5 protein expression in the five cell lines. (C-D) qPCR of STX5 mRNA expression in Huh7 and PLC/PRF/5 cells transduced with LV-shSTX5 and negative control LV-NC for 24 h. (E) qPCR of STX5 mRNA expression in MHCC97H cells transduced with OE-STX5 and negative control vector for 24 h. (F-G) Western blot analysis of STX5 protein expression in Huh7 and PLC/PRF/5 cells transduced with LV-shSTX5 and the LV-NC negative control for 24. (H) Western blot analysis of STX5 protein expression in MHCC97H cells transduced with OE-STX5 and negative control vector for 24 h. (I) Colony formation assay of the growth of Huh7 cells transduced with LV-shSTX5 and the negative control LV-NC over a 2-week period. (J-K) Detection of changes in E-cadherin, N-cadherin, and Snail protein levels in Huh7 and PLC/PRF/5 cells transduced with LV-shSTX5 and LV-NC and in MHCC97H cells transfected with OE-STX5 and the vector. (L-N) Comparison of migration in Huh7, PLC/PRF/5, and MHCC97H cells using Transwell chambers. (O-P) Comparison of the adhesion of Huh7, PLC/PRF/5, and MHCC97H cells to the extracellular matrix. (Q-S) Wound healing assays to compare the motility of the Huh7, PLC/PRF/5, and MHCC97H cell lines. Data are means ± SD of three independent assays. *$p<0.05$, **$p<0.01$, ***$p<0.001$, ****$p<0.0001$. qPCR, quantitative polymerase chain reaction; EMT, epithelial-mesenchymal transition.

ral vectors containing shRNA sequences targeting STX5 to knock down STX5 expression. The best efficiency of knockdown was observed with LV-shSTX5 (Fig. 2C, D, F, G). The next step was to examine the impact of STX5 on HCC cell adhesion, migration, and EMT in MHCC97H cells, which have low levels of endogenous STX5 (Fig. 2A, B). Overexpression of STX5 was observed in MHCC97H cells transfected with OE-STX5, demonstrating excellent overexpression efficiency (Fig. 2E, H).

We studied the effects of STX5 overexpression and inhibition on HCC cell adhesion, migration, and EMT. STX5 overexpression caused a significant increase in migration (Fig. 2N, S) in the MHCC97H cell line, which was consistent with the increased expression of N-cadherin and reduced E-cadherin protein (Fig. 2K). Conversely, a significant decrease in migration and a significant increase in adhesion were observed Huh7 and PLC/PRF/5 cells following STX5 suppression by lentiviral transduction (Fig. 2L, M, O, P), which was consistent with the reduced expression of N-cadherin and increased E-cadherin protein (Fig. 2J). In addition, the inhibition of STX5 significantly reduced the proliferation of Huh7 (Fig. 2I).

STX5 regulates the PI3K/mTOR pathway

We performed transcriptome sequencing in Huh7 cells transfected with OE-STX5 and negative control vectors, and differentially expressed genes (DEGs) were identified (Fig. 3A, B). The results of enrichment analysis of the DEGs in the OE-STX5 and vector groups showed that in the aspect of biological processes, the DEGs were mainly enriched in the terms cell adhesion and epithelial cell migration (Fig. 3C). According to DisGeNET analysis, DEGs were significantly enriched in liver cirrhosis, liver diseases, and fatty liver (Fig. 3D). DEGs were also enriched in the Golgi lumen (Fig. 3E). KEGG pathway enrichment analysis showed that the DEGs were enriched in the PI3K/Akt and mTOR pathways and also in proliferation-related pathways, such as the nuclear factor kappa B (NF-κB) and JAK-STAT pathways (Fig. 3F). GSEA showed that STX5 expression had a significant positive correlation with mTOR signaling in HCC (Fig. 3G).

Western blot analysis showed that the levels of PI3K 110β and phospho-mTOR (p-mTOR) in Huh7 and PLC/PRF/5 cells decreased significantly after STX5 knock down by the lentiviral vector for 24 h (Fig. 3H). Conversely, the levels of p-PI3K, mTOR, and p-mTOR were increased in MHCC97H cells at 24 h after STX5 overexpression (Fig. 3I). The data suggest that STX5 is a PI3K/mTOR pathway regulator, in keeping with our RNA-seq and GSEA data.

Effects of STX5 expression levels on HCC cell adhesion and migration via the PI3K/mTOR pathway

The 1nM concentration of rapamycin can significantly inhibit the expression of p-MTOR in huh7 after STX5 knockdown (Fig. 4A). When cells interacted with rapamycin, a PI3K/mTOR inhibitor, STX5 inhibition-mediated antimetastasis was enhanced. The effects of STX5 expression levels on HCC cell adhesion and migration were exerted via the PI3K/mTOR pathway. We studied the effect of inhibition or induction of PI3K/mTOR signal pathway caused by STX5 overexpression or inhibition on the adhesion and migration of HCC cells. We found that STX5 overexpression with a plasmid led to increased cell migration and inhibited cell adhesion. In addition, STX5-mediated metastasis was reversed when cells were cotreated with rapamycin (Fig. 4B, D, F). As a consequence, our results showed that STX5 overexpression inhibited HCC cell adhesion and promoted migration via the PI3K/mTOR pathway.

Dual inhibition of STX5 and mTOR exerts cooperative antimetastatic effects on HCC cells

After observing the association between STX5 and mTOR, we explored whether combining STX5 and mTOR targeting enhanced HCC cell migration and inhibited cell adhesion. We observed that the combination of rapamycin, an mTOR inhibitor, and STX5 suppression contributed to more notably enhanced suppression of HCC cell migration and adhesion promotion than treatment with rapamycin alone or STX5 suppression alone (Fig. 4C, E, G). We observed significant inhibitory effects on HCC cells derived from STX5 and mTOR combined suppression.

STX5 knockdown inhibits HCC cell metastasis in vivo

Sequentially we studied the antimetastatic effects of STX5 inhibition *in vivo* in a lateral tail vein model of metastasis. Compared with nude mice inoculated with LV-shNC Huh7 cells, nude mice inoculated with Huh7 LV-shSTX5 cells exhibited significantly reduced lung metastasis, liver metastasis, and tumor burden (Fig. 5A, B), indicating that the metastatic ability of Huh7 cells decreased significantly after knockdown of STX5. Importantly, the IHC staining data showed positive AFP staining in metastatic nodules (Fig. 5C, D), further confirming that the nodules originated in HCC cells. The expression of STX5, N-cadherin, and E-cadherin in lung and liver tissues was also detected by IHC staining. The expression of AFP and N-cadherin was more obviously decreased and the expression of E-cadherin was increased in the Huh7 LV-shSTX5 group compared with the Huh7 LV-shNC group (Fig. 5C, D). Thus, STX5 inhibition inhibited metastatic growth *in vivo*, confirming the *in vitro* finding.

Discussion

Using large independent datasets and our cohort of patients, we verified that STX5 expression was significantly enhanced in HCC tissues compared with non-tumor liver tissues. Clinically, the overexpression of STX5 in HCC patients was significantly correlated with elevated AFP level, hepatitis B virus (HBV) infection status, tumor number, body mass index, and other invasive tumor characteristics. In addition, the expression level of STX5 in HCC was an independent predictor of OS and DFS in HCC patients, and HCC patients with high STX5 expression had a poorer prognosis than HCC patients with low STX5 expression. Functionally, STX5 regulated adhesion and EMT at least partially through the PI3K/mTOR pathway, thus controlling the migration and metastasis of HCC cells. Dual inhibition of STX5 and mTOR cooperatively promoted the adhesion of HCC cells, inhibited EMT, and had a synergistic antimetastatic effect (Fig. 6). In summary, our *in vitro* and *in vivo* results demonstrate an antimetastasis effect of STX5 inhibition and are relevant to our clinical observation that high STX5 expression is associated with more aggressive characteristics and poorer survival.

The role of STX5 in cancer development remains unknown. In mammals, STX5 mediates endoplasmic reticulum to Golgi and retrograde transport from Golgi to endoplasmic reticulum. It has an important role in eukaryotic cell secretion pathways and has been implicated in infections and neurodegenerative diseases.[18] Linders *et al*.[19] recently described congenital glycosylation disorders caused by site-specific mutations in the N-terminus of STX5. In addition, recent studies have shown that Beclin 2 interacts with STX5 and STX6 to promote the fusion of MEKK3- or TAK1-related ATG9A+ vesicles with phages and their subsequent degradation, negatively regulating tumorigenesis. The finding suggests that STX5 is

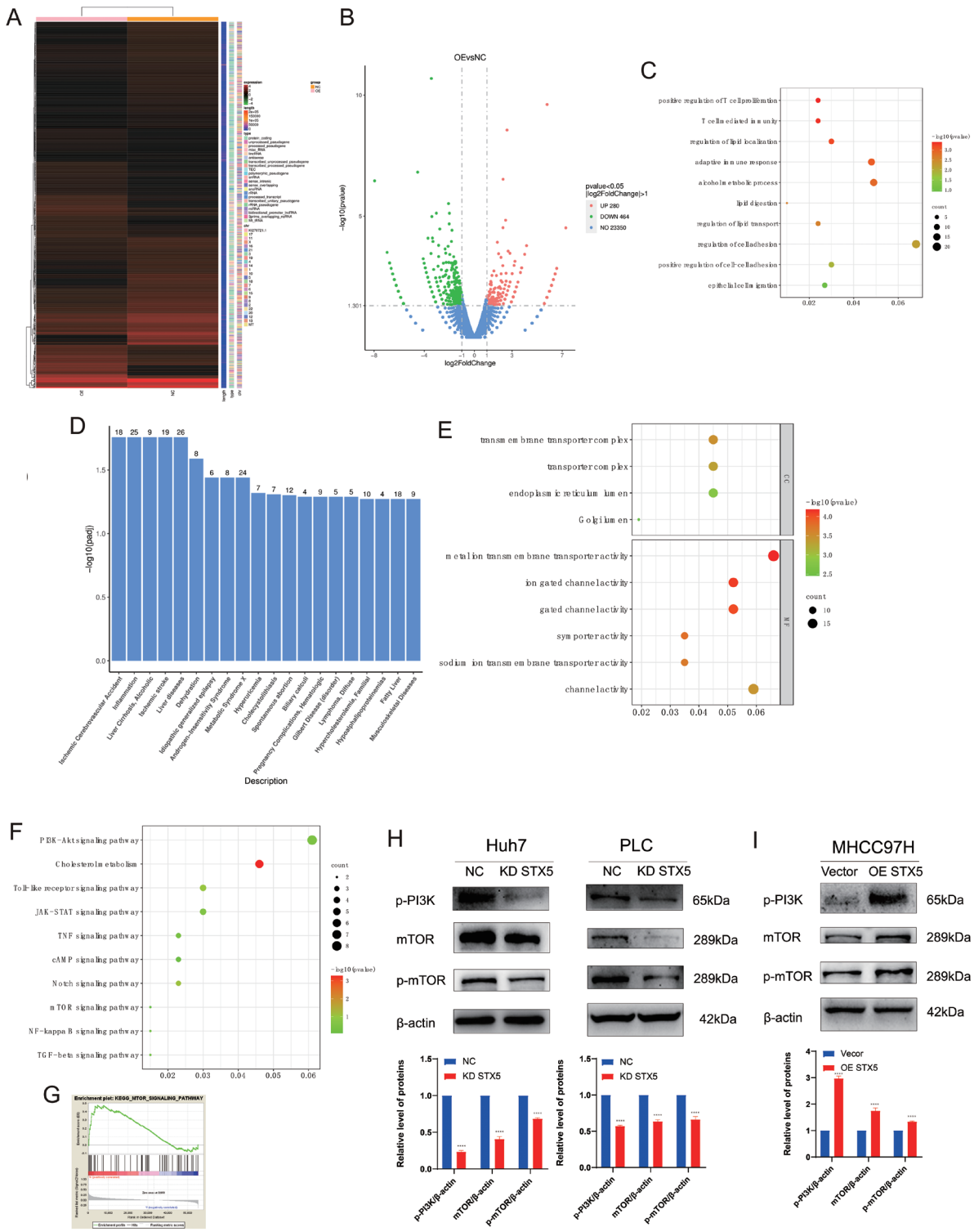

Fig. 3. STX5 is a regulator of the PI3K/mTOR pathway. Transcriptome sequencing and functional enrichment analysis of the vector and OE-STX5 groups. (A) Heatmap showing the DEGs in the OE-STX5 and vector groups. DEGs with similar expression patterns are grouped. Differences in the color of two squares in each row reflects differences in gene expression. (B) Red dots on the volcano plot represent upregulated genes. Green dots represent downregulated genes in the OE-STX5 group compared with the vector group. (C-F) Results of enrichment analyses of the DEGs between the OE-STX5 and vector groups, i.e. biological process, cellular component, molecular function, KEGG pathway, and DisGeNET enrichment analyses. (G) A positive association between STX5 expression and the MTOR signaling pathway in HCC was demonstrated by GSEA. (H-I) Western blot assays of p-PI3K, p-mTOR, and mTOR protein levels in Huh7 and PLC/PRF/5 cells transduced with LV-shSTX5 and LV-NC and in MHCC97H cells transfected with OE-STX5 and the vector for 24 h. Data are means ± SD of three independent assays. *p<0.05, **p<0.01, ***p<0.001, ****p<0.0001. GSEA, Gene Set Enrichment Analysis; KEGG, Kyoto Encyclopedia of Genes and Genomes.

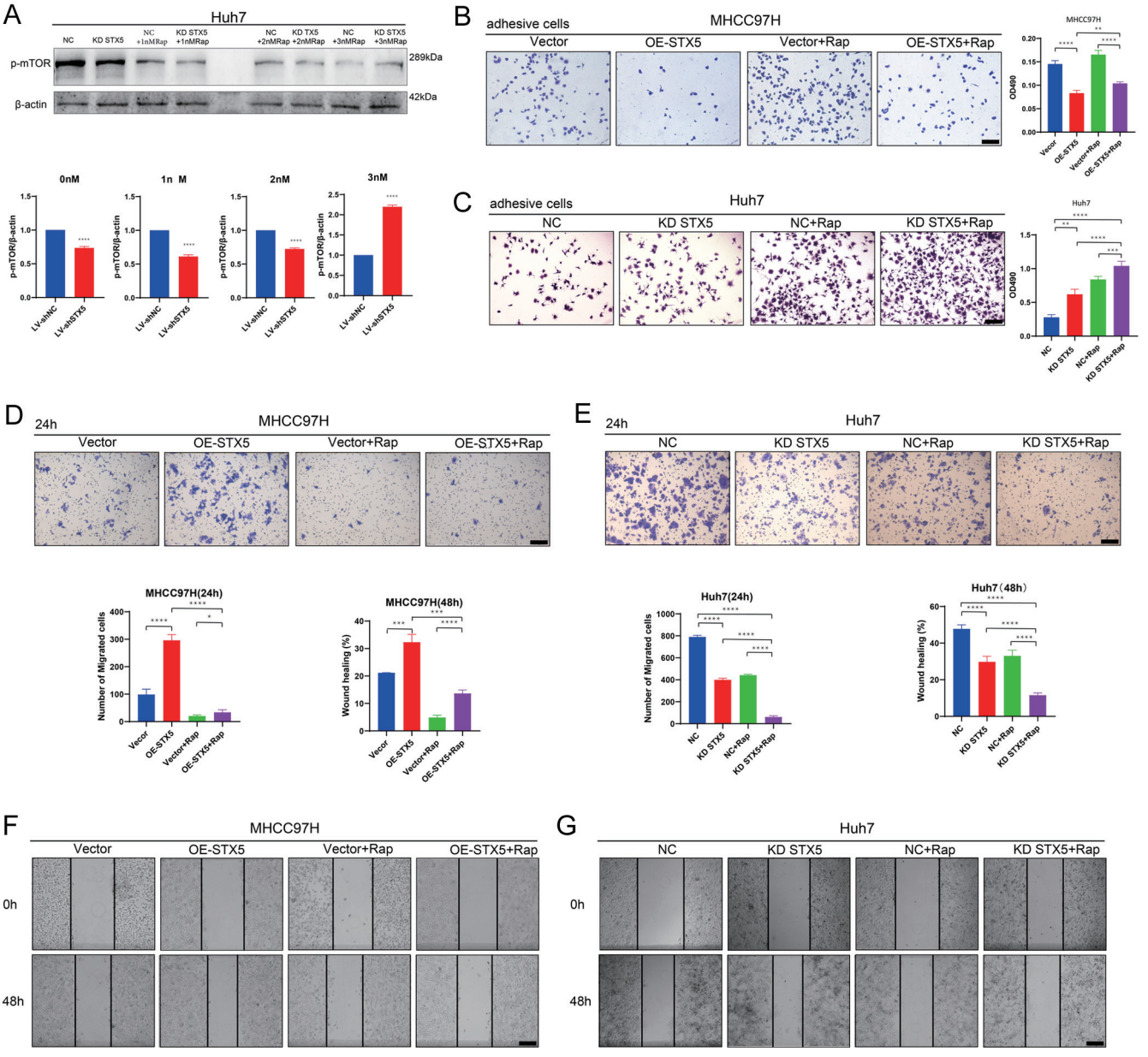

Fig. 4. Effects of STX5 expression on HCC cell adhesion and migration via the mTOR pathway. (A) Screening was performed to determine the optimal concentration of rapamycin for mTOR pathway inhibition. (B, C) Adhesion of Huh7 cells transduced with LV-shSTX5 or OE-STX5, treated with PBS (control) or rapamycin (1 nM), or both transfected and treated for 24 h. was compared. (D, E) Transwell chambers were used to compare the invasion and migration of Huh7 cells. (F, G) *In vitro* wound healing assays compared Huh7 cell motility. Data are means ± SD of three independent assays. *p<0.05, **p<0.01, ***p<0.001, ****p<0.0001.

related to tumor development. STX5 is expressed as long (42 kDa) and short (35 kDa) isoforms.[20] The short isoform (STX5S) is concentrated in the Golgi apparatus, and the long isoform (STX5L) is present in both the Golgi apparatus and endoplasmic reticulum. Although STX5S localized in the Golgi apparatus has been extensively studied, little is known about STX5L. Moreover, although STX5S and STX5L share an amino acid sequence of considerable length, they appear to have different roles in regulating the metabolism and transport of beta-amyloid precursor protein in the early secretory apparatus.[21] Our study showed that STX5L promoted the development of HCC.

STX5 promotes metastasis by inhibiting tumor cell adhesion. The extracellular stroma is a complex network of cell-secreted macromolecules, including collagens, enzymes, and glycoproteins, whose primary function is to support the structural scaffolding and biochemical functions of cells and tissues. In contrast, continuous modification or degradation of the extracellular matrix may lead to pathological conditions. During tumor development, epithelial tumor cells may undergo EMT.[22–26] The process enhances the ability of cancer cells to detach from the primary tumor and invade and is critical for the spread and metastasis of cancer cells.[27–31] Matrix metalloproteinases and multiple adhesion receptors are involved in transfer-related ECM modification, and integrins also play a crucial role.[32] Cells adhere to

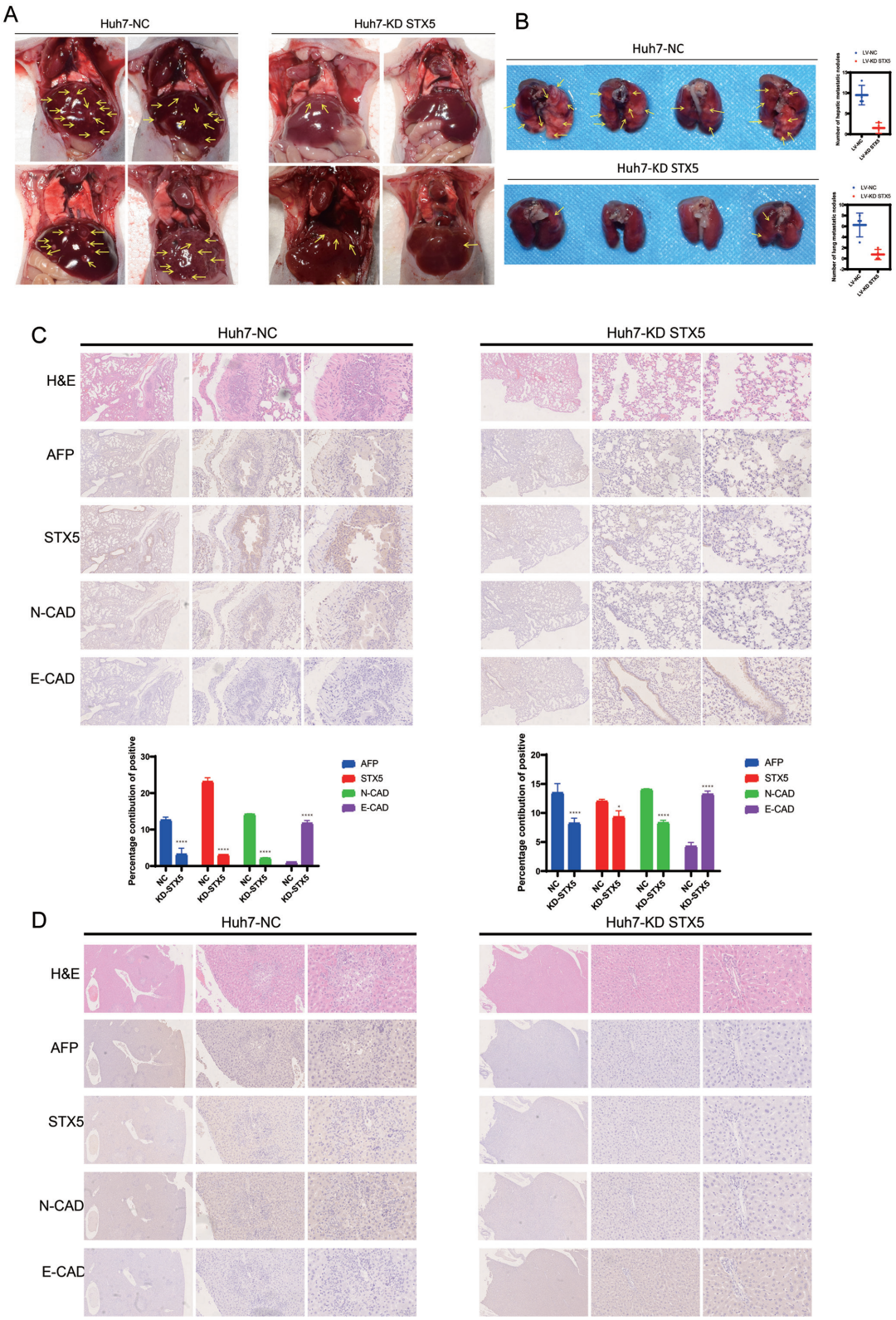

Fig. 5. STX5 knockdown inhibits HCC cell metastasis *in vivo*. Nude mice (n=5) were injected with 2 × 10^6 LV-shNC or LV-shSTX5 Huh7 cells suspended in 200 μL of PBS via the tail vein. (A) Representative images of hepatic tissues from nude mice. (B) Representative images of lung tissues from nude mice. (C) Hematoxylin and eosin and IHC staining of AFP, STX5, E-cadherin, and N-cadherin in lung tissue. (D) Hematoxylin and eosin and IHC staining of AFP, STX5, E-cadherin, and N-cadherin in liver tissue. AFP, alpha-fetoprotein; IHC, Immunohistochemical.

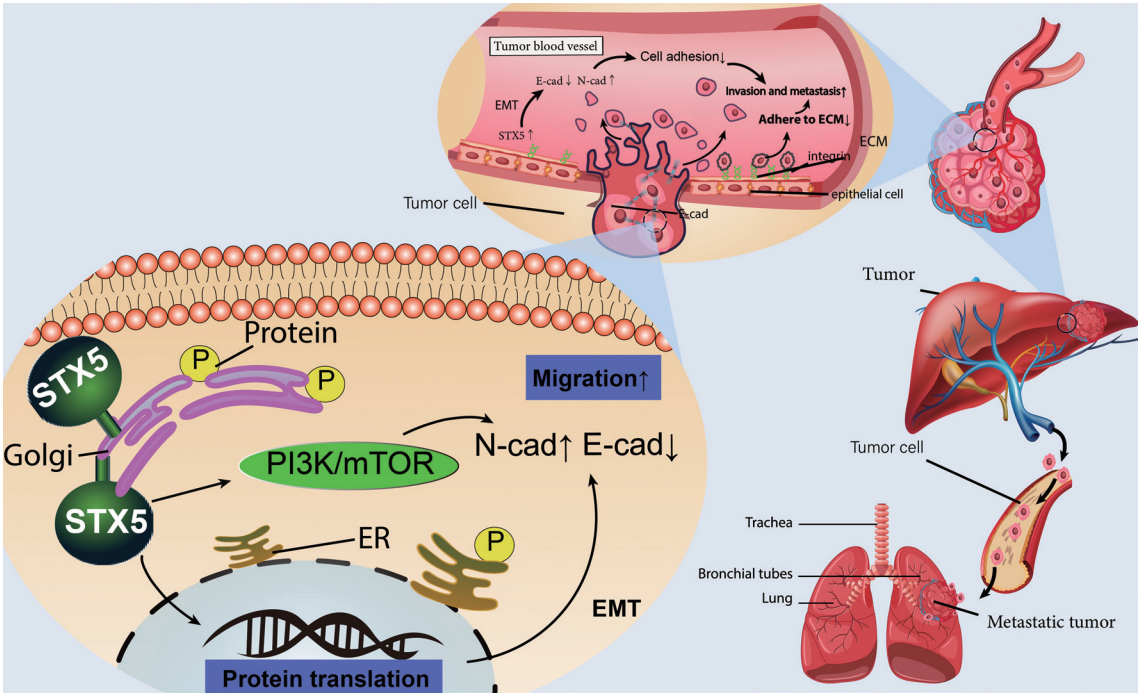

Fig. 6. Diagram of the mechanism of STX5 involvement in HCC metastasis. Nomogram based on STX5 expression level to predict 1-year, 3-year, and 5-year survival rates of HCC patients, difference in expression, and functional phenotype of STX5 in hepatocellular carcinoma cells and regulation of the PI3K/mTOR signaling pathway by STX5, an important molecular target of drug therapy of liver cancer recurrence and metastasis.

each other and/or the surrounding matrix. In normal cells, the regulation of cell-to-cell (intercellular) and cell-to-matrix adhesion is tightly controlled, but most human cancers have defects in cell adhesion. Multilateral communication between tumor cells, extracellular matrix, and adjacent cells is achieved through adhesion molecules, extracellular matrix components, proteolytic enzymes, and endogenous inhibitors. There is ample evidence that reduced adhesion is characteristic of tumor cells during tumor development. Tumor cells gain the ability to change their shape, separate, and move through spaces that disrupt normal tissue structure. The acquisition of this function is mediated by changes in the expression of adhesion molecules and/or increased levels of secreted proteolytic enzymes, including matrix metalloproteinases.[33] Our study shows that STX5 reduced the adhesion between HCC cells and to the extracellular matrix, promoted tumor cell shedding from the primary site, and thus promoted tumor metastasis. By bioinformatic analysis, we further found that STX5 is closely related to distant metastasis. However, during metastasis initiation, enhancing the adhesion ability of tumor cells benefits tumor progression. For example, collagen cross-linking increases the adhesion of bone marrow cells and produces a microenvironment conducive to disseminated tumor cell colonization.[34] The effect may relate the presence of specific adhesion receptors in different metastatic sites. For example, exogenous integrins α6β4 and α6β1 are associated with lung metastasis, and exogenous integrin αvβ5 is associated with liver metastasis.[35]

STX5 mediated HCC cell adhesion, migration, and EMT through the PI3K/mTOR pathway. The PI3K/mTOR pathway regulates cell proliferation, growth, size, metabolism, and motility.[36–39] The genes that compose this pathway have been extensively studied and found to be universally activated in human cancers.[40,41] Interestingly, PI3K is also involved in the adhesion signal transduction pathway, which is consistent with the conclusion that STX5 mediates HCC cell adhesion through the PI3K/mTOR pathway found in our study. However, the mechanism by which the PI3K/mTOR pathway affects adhesion and metastasis, which may occur due to its regulation of autophagy, needs further study. Indeed, some studies have shown that PI3K/mTOR inhibits liver cancer metastasis by inducing autophagy.[1]

There are some limitations in the study. Since HCC is most commonly associated with intrahepatic metastasis, injecting tumor cells through the caudal vein cannot perfectly simulate HCC cell metastasis.

Acknowledgments

We thank American Journal Experts for the editorial assistance.

Funding

Natural Science Foundation of Shandong Province (CN) (ZR201911030198).

Conflict of interest

The authors have no conflict of interests related to this publication.

Author contributions

Contributed to the preparation of this manuscript (all authors), responsible for confirming the topic (BZ), responsible for writing the first draft of this article (BZ, ZZ, YW), contributed to furtherly editing and polishing the manuscript (TG, MH). approved the final manuscript (all authors).

Ethical statement

Collection of samples used in this study was approved by the Ethics Committee of the Affiliated Hospital of Qingdao University.

Data sharing statement

The qPCR, western blot, and other data used to support the findings of this study are included within the article.

References

[1] Zhang M, Liu S, Chua MS, Li H, Luo D, Wang S, *et al*. Correction: SOCS5 inhibition induces autophagy to impair metastasis in hepatocellular carcinoma cells via the PI3K/Akt/mTOR pathway. Cell Death Dis 2019;10(11):799. doi:10.1038/s41419-019-2009-z, PMID:31641102.

[2] Bray F, Ferlay J, Soerjomataram I, Siegel RL, Torre LA, Jemal A. Global cancer statistics 2018: GLOBOCAN estimates of incidence and mortality worldwide for 36 cancers in 185 countries. CA Cancer J Clin 2018;68(6):394–424. doi:10.3322/caac.21492, PMID:30207593.

[3] Sung H, Ferlay J, Siegel RL, Laversanne M, Soerjomataram I, Jemal A, *et al*. Global Cancer Statistics 2020: GLOBOCAN Estimates of Incidence and Mortality Worldwide for 36 Cancers in 185 Countries. CA Cancer J Clin 2021;71(3):209–249. doi:10.3322/caac.21660, PMID:33538338.

[4] Wang W, Wei C. Advances in the early diagnosis of hepatocellular carcinoma. Genes Dis 2020;7(3):308–319. doi:10.1016/j.gendis.2020.01.014, PMID:32884985.

[5] Tabrizian P, Jibara G, Shrager B, Schwartz M, Roayaie S. Recurrence of hepatocellular cancer after resection: patterns, treatments, and prognosis. Ann Surg 2015;261(5):947–955. doi:10.1097/SLA.0000000000000710, PMID:25010665.

[6] Wickner W, Schekman R. Membrane fusion. Nat Struct Mol Biol 2008;15(7):658–664. doi:10.1038/nsmb.1451, PMID:18618939.

[7] Bock JB, Matern HT, Peden AA, Scheller RH. A genomic perspective on membrane compartment organization. Nature 2001;409(6822):839–841. doi:10.1038/35057024, PMID:11237004.

[8] Jahn R, Lang T, Sudhof TC. Membrane fusion. Cell 2003;112(4):519–533. doi:10.1016/s0092-8674(03)00112-0, PMID:12600315.

[9] Chao DS, Hay JC, Winnick S, Prekeris R, Klumperman J, Scheller RH. SNARE membrane trafficking dynamics in vivo. J Cell Biol 1999;144(5):869–881. doi:10.1083/jcb.144.5.869, PMID:10085287.

[10] Hui N, Nakamura N, Sonnichsen B, Shima DT, Nilsson T, Warren G. An isoform of the Golgi t-SNARE, syntaxin 5, with an endoplasmic reticulum retrieval signal. Mol Biol Cell 1997;8(9):1777–1787. doi:10.1091/mbc.8.9.1777, PMID:9307973.

[11] Dascher C, Matteson J, Balch WE. Syntaxin 5 regulates endoplasmic reticulum to Golgi transport. J Biol Chem 1994;269(47):29363–29366. PMID:7961911.

[12] Hay JC, Klumperman J, Oorschot V, Steegmaier M, Kuo CS, Scheller RH. Localization, dynamics, and protein interactions reveal distinct roles for ER and Golgi SNAREs. J Cell Biol 1998;141(7):1489–1502. doi:10.1083/jcb.141.7.1489, PMID:9647643.

[13] Suga K, Hattori H, Saito A, Akagawa K. RNA interference-mediated silencing of the syntaxin 5 gene induces Golgi fragmentation but capable of transporting vesicles. FEBS Lett 2005;579(20):4226–4234. doi:10.1016/j.febslet.2005.06.053, PMID:16081076.

[14] Shestakova A, Suvorova E, Pavliv O, Khaidakova G, Lupashin V. Interaction of the conserved oligomeric Golgi complex with t-SNARE Syntaxin5a/Sed5 enhances intra-Golgi SNARE complex stability. J Cell Biol 2007;179(6):1179–1192. doi:10.1083/jcb.200705145, PMID:18086915.

[15] Renna M, Schaffner C, Winslow AR, Menzies FM, Peden AA, Floto RA, *et al*. Autophagic substrate clearance requires activity of the syntaxin-5 SNARE complex. J Cell Sci 2011;124(Pt 3):469–482. doi:10.1242/jcs.076489, PMID:21242315.

[16] Kroemer G, Jaattela M. Lysosomes and autophagy in cell death control. Nat Rev Cancer 2005;5(11):886–897. doi:10.1038/nrc1738, PMID:16239905.

[17] Rabinowitz JD, White E. Autophagy and metabolism. Science 2010;330(6009):1344–1348. doi:10.1126/science.1193497, PMID:21127245.

[18] Linders PT, Horst CV, Beest MT, van den Bogaart G. Stx5-Mediated ER-Golgi Transport in Mammals and Yeast. Cells 2019;8(8):780. doi:10.3390/cells8080780, PMID:31357511.

[19] Zhu M, Deng G, Tan P, Xing C, Guan C, Jiang C, *et al*. Beclin 2 negatively regulates innate immune signaling and tumor development. J Clin Invest 2020;130(10):5349–5369. doi:10.1172/JCI133283, PMID:32865519.

[20] Miyazaki K, Wakana Y, Noda C, Arasaki K, Furuno A, Tagaya M. Contribution of the long form of syntaxin 5 to the organization of the endoplasmic reticulum. J Cell Sci 2012;125(Pt 23):5658–5666. doi:10.1242/jcs.105304, PMID:23077182.

[21] Suga K, Saito A, Tomiyama T, Mori H, Akagawa K. The Syntaxin 5 isoforms Syx5 and Syx5L have distinct effects on the processing of {beta}-amyloid precursor protein. J Biochem 2009;146(6):905–915. doi:10.1093/jb/mvp138, PMID:19720618.

[22] Dongre A, Weinberg RA. New insights into the mechanisms of epithelial-mesenchymal transition and implications for cancer. Nat Rev Mol Cell Biol 2019;20(2):69–84. doi:10.1038/s41580-018-0080-4, PMID:30459476.

[23] Savagner P. The epithelial-mesenchymal transition (EMT) phenomenon. Ann Oncol 2010;21(Suppl 7):vii89–92. doi:10.1093/annonc/mdq292, PMID:20943648.

[24] Yang J, Antin P, Berx G, Blanpain C, Brabletz T, Bronner M, *et al*. Guidelines and definitions for research on epithelial-mesenchymal transition. Nat Rev Mol Cell Biol 2020;21(6):341–352. doi:10.1038/s41580-020-0237-9, PMID:32300252.

[25] Kalluri R. EMT: when epithelial cells decide to become mesenchymal-like cells. J Clin Invest 2009;119(6):1417–1419. doi:10.1172/JCI39675, PMID:19487817.

[26] Chaffer CL, San Juan BP, Lim E, Weinberg RA. EMT, cell plasticity and metastasis. Cancer Metastasis Rev 2016;35(4):645–654. doi:10.1007/s10555-016-9648-7, PMID:27878502.

[27] Nieto MA, Huang RY, Jackson RA, Thiery JP. Emt: 2016. Cell 2016;166(1):21–45. doi:10.1016/j.cell.2016.06.028, PMID:27368099.

[28] Quail DF, Joyce JA. Microenvironmental regulation of tumor progression and metastasis. Nat Med 2013;19(11):1423–1437. doi:10.1038/nm.3394, PMID:24202395.

[29] Thiery JP, Acloque H, Huang RY, Nieto MA. Epithelial-mesenchymal transitions in development and disease. Cell 2009;139(5):871–890. doi:10.1016/j.cell.2009.11.007, PMID:19945376.

[30] Tsai JH, Donaher JL, Murphy DA, Chau S, Yang J. Spatiotemporal regulation of epithelial-mesenchymal transition is essential for squamous cell carcinoma metastasis. Cancer Cell 2012;22(6):725–736. doi:10.1016/j.ccr.2012.09.022, PMID:23201165.

[31] Tsai JH, Yang J. Epithelial-mesenchymal plasticity in carcinoma metastasis. Genes Dev 2013;27(20):2192–2206. doi:10.1101/gad.225334.113, PMID:24142872.

[32] Paolillo M, Schinelli S. Extracellular Matrix Alterations in Metastatic Processes. Int J Mol Sci 2019;20(19):4947. doi:10.3390/ijms20194947, PMID:31591367.

[33] Bourboulia D, Stetler-Stevenson WG. Matrix metalloproteinases (MMPs) and tissue inhibitors of metalloproteinases (TIMPs): Positive and negative regulators in tumor cell adhesion. Semin Cancer Biol 2010;20(3):161–168. doi:10.1016/j.semcancer.2010.05.002, PMID:20470890.

[34] Altorki NK, Markowitz GJ, Gao D, Port JL, Saxena A, Stiles B, *et al*. The lung microenvironment: an important regulator of tumour growth and metastasis. Nat Rev Cancer 2019;19(1):9–31. doi:10.1038/s41568-018-0081-9, PMID:30532012.

[35] Hoshino A, Costa-Silva B, Shen TL, Rodrigues G, Hashimoto A, Tesic Mark M, *et al*. Tumour exosome integrins determine organotropic metastasis. Nature 2015;527(7578):329–335. doi:10.1038/nature15756, PMID:26524530.

[36] Fruman DA, Chiu H, Hopkins BD, Bagrodia S, Cantley LC, Abraham RT. The PI3K Pathway in Human Disease. Cell 2017;170(4):605–635. doi:10.1016/j.cell.2017.07.029, PMID:28802037.

[37] Jafari M, Ghadami E, Dadkhah T, Akhavan-Niaki H. PI3k/AKT signaling pathway: Erythropoiesis and beyond. J Cell Physiol 2019;234(3):2373–2385. doi:10.1002/jcp.27262, PMID:30192008.

[38] Saxton RA, Sabatini DM. mTOR Signaling in Growth, Metabolism, and Disease. Cell 2017;168(6):960–976. doi:10.1016/j.cell.2017.02.004, PMID:28283069.

[39] Manning BD, Toker A. AKT/PKB Signaling: Navigating the Network. Cell 2017;169(3):381–405. doi:10.1016/j.cell.2017.04.001, PMID:28431241.

[40] Alzahrani AS. PI3K/Akt/mTOR inhibitors in cancer: At the bench and bedside. Semin Cancer Biol 2019;59:125–132. doi:10.1016/j.semcancer.2019.07.009, PMID:31323288.

[41] Papa A, Pandolfi PP. The PTEN(-)PI3K Axis in Cancer. Biomolecules 2019;9(4):153. doi:10.3390/biom9040153, PMID:30999672.